Available online at www.sciencedirect.com

SCIENCE DIRECT®

European Polymer Journal 39 (2003) 1831–1838

EUROPEAN POLYMER JOURNAL

www.elsevier.com/locate/europolj

Experimental determination of rheological properties of polydimethylsiloxane

L. Di Landro [a,*], M. Levi [a], D. Nichetti [b], A. Consolo [a]

[a] *Dipartimento di Chimica, Materiali e Ingegneria Chimica, Politecnico di Milano, "G. Natta", Piazza L. da Vinci 32, 20133 Milano, Italy*

[b] *Chiorino S.p.A., Via S. Agata 9, 13900 Biella, Italy*

Received 4 February 2003; received in revised form 25 March 2003; accepted 11 April 2003

Abstract

A series of linear polydimethylsiloxane of different molecular weight and with reduced polydispersity were prepared by partial fractionation of commercial products. The rheological functions, i.e. zero shear viscosity (η_0), first and second normal stress coefficients (Ψ_{10} and Ψ_{20}), of the materials were experimentally measured by conventional rotational rheometers and by a rotation rod apparatus. The relationships between molecular structure (molecular weight and polydispersity index) and rheological functions are presented and discussed on the basis of equations proposed in the literature. Zero shear viscosity data conform to the well-known dependence on a power 3.5 of molecular weight. However, a consistently stronger influence of molecular weight over Ψ_{10} and Ψ_{20} is found. The influence of polydispersity over Ψ_{10} is also analyzed.

Keywords: Shear viscosity; Normal stresses; Weissenberg effect; Poly(dimethylsiloxane); Molecular weight dependence

1. Introduction

The rheological behavior of high polymer melts is typically characterized by non-Newtonian response to imposed shear rate. Due to the presence of entanglements between chains, the fluid behavior becomes markedly viscoelastic and, even in isothermal, steady shear flow conditions, normal stresses arise, whose intensity depends on the molecular structure of the polymeric material. Therefore the characterization of the rheological properties of such liquids requires the determination of three independent functions of shear rate ($\dot{\gamma}$), that is the shear stress τ, the first (N_1) and the second (N_2) normal stress differences (or, alternatively, the shear viscosity (η), the first ($\Psi_1 = N_1/\dot{\gamma}^2$) and the second ($\Psi_2 = N_2/\dot{\gamma}^2$) normal stress coefficients) [1,2]. In many polymer processing designing procedures, simplified constitutive equations are adopted, which often neglect or assume a priori estimates of normal stresses. However, such stresses may have strong influence over a number of phenomena relevant for polymer processing, such as, for instance, extruded swelling or flow instabilities [1,2]. The knowledge of the flow functions dependence on molecular structure of polymer melts and solutions can thus furnish a better insight into the mechanisms of molecular dynamics on one hand, and also from a technological point of view, more reliable rheological constitutive equations and material properties relationships should help to improve the design capability of polymer processing equipment, when material flow is involved.

Surely the most important and most studied of the rheological properties of polymeric fluids is the shear viscosity. Polymer melts are characterized by high viscosity values, which largely depend on shear rate, often

---

[*] Corresponding author. Tel.: +39-2-2399-3253; fax: +39-2-7063-8173.

E-mail address: luca.dilandro@polimi.it (L. Di Landro).

0014-3057/$ - see front matter © 2003 Elsevier Ltd. All rights reserved.
doi:10.1016/S0014-3057(03)00104-6

exhibiting variation as large as two or three orders of magnitude. The dependence of the zero shear viscosity (η_0) of a polymer on the molecular weight (M) was extensively investigated in the past. An exponential functional dependence $\eta_0 \propto M^\alpha$ is generally accepted. Values of $\alpha = 1$ for M below a critical value M_c, when no entanglements are effective between short chains, and $\alpha = 3.4$–3.5 for $M > M_c$ are usually consistent with experimental data [3,4]. In the case of polydisperse polymers, Locati and Gargani proposed an equation, which relates η_0 to the weight average molecular weight $\overline{M}_w$ and to the polydispersity index $I = \overline{M}_w/\overline{M}_n$ [5]:

$$\eta_0 = k\overline{M}_w^\alpha \cdot I^\delta \tag{1}$$

Values of $\delta \simeq 0.5$ were found to adequately describe the experimental results of polyethylenes in a wide range of molecular weights and polydispersities. Based on the superposition of the rheological behavior of monodisperse fractions, models predicting the zero and the shear rate dependence of viscosity for polydisperse materials were later proposed [6,7].

Few studies are reported on the dependence of the first normal stress function (Ψ_1) on molecular weight and polydispersity [4,8–10]. Normal stresses are expression of the viscoelastic character of polymer melts and solutions and a strong dependence on $\overline{M}_w$ is therefore expected as $\overline{M}_w$ exceeds the critical value M_c. Gao et al. [9], operating with narrow molecular weight distribution polystyrene solutions, found a dependence of the zero shear first normal stress coefficient (Ψ_{10}) on a power 6.8–7.8 of molecular weight. For linear polymers, with high molecular tails, Minoshima et al. [10] proposed the following expression:

$$\Psi_{10} = k'\overline{M}_w^{2\alpha} \cdot I^\alpha \tag{2}$$

where k' is a constant for a given material and temperature, $\overline{M}_w$ is the weight average molecular weight, $I = \overline{M}_w/\overline{M}_n$ is the polydispersity index and α is equal to 3.4. It can be observed from Eqs. (1) and (2) that, while the influence of I on shear viscosity is relatively limited, a strong dependence of the first stress coefficient on both $\overline{M}_w$ and I is to be expected.

Probably due to the experimental difficulty in measuring the second normal stress difference N_2, even less studied is the influence of polymer structure on the second normal stress coefficient Ψ_{20}. As a matter of facts, while a number of experimental techniques are available for the measurement of shear viscosity and the first normal stress difference as function of shear rate, more difficult is to obtain reliable experimental results for N_2. Gao et al., in the work already cited [9], by using a modified cone-plate rheometer, estimated Ψ_{20} for a number of polystyrene solutions of different $\overline{M}_w$ and I, although a clear functional dependence could not be established on the basis of experimental data. Using the Doi–Edwards model, Marrucci and Grizzuti [11] showed that, for monodisperse polymers in slow shear flow, Ψ_{20} should be proportional to the square of the characteristic relaxation time and, therefore, to $M^{2\alpha}$. A relationship of the type $\Psi_{20} \propto M^{2\alpha}$ should therefore be expected with constant Ψ_{20}/Ψ_{10} ratio. No indication is available for the polydispersity dependence of Ψ_{20}.

Based on the Weissenberg effect, the rotating rod rheometer, in combination with an independent method for the experimental determination of the first normal stress coefficient, is an alternative, convenient device for the measurement of second normal stress coefficient at low shear rates [12–14]. In this research the relationship between material molecular parameters such as molecular weight and polydispersity on the rheological parameters (η_0, Ψ_{10}, Ψ_{20}) of a series of linear polydimethylsiloxane (PDMS), were experimentally investigated and their relationship with material molecular parameters such as molecular weight and polydispersity is discussed.

1.1. Rotational rod rheometer

When a rod rotates in a large volume of a viscoelastic fluid, the free surface on the fluid is deformed as a consequence of the normal stresses induced by the shearing motion. This free surface deformation in the concentric cylinder geometry is usually known as Weissenberg effect [15]. A schematic representation is shown in Fig. 1. The theory of rod climbing, analyzing the equations of motion via a perturbation theory, could correlate the height of climb to the rheological properties of the fluid in slow rotational regime, provided the shear rate is sufficiently low, so that shear viscosity, first and second normal stress coefficients do not depart from their low shear rate values [2]. Using this approximation, a viscoelastic material can be described by a second-order fluid constitutive equation, in which the parameters are the shear viscosity η_0 and the two normal stress coefficients, Ψ_{10} and Ψ_{20}. The theoretical analysis, in the case of small rod diameter and negligible inertial effects, shows that the fluid level at the rod surface rises to a height:

$$h(R,\Omega^2) - h_0 = \frac{R}{2\sqrt{\gamma\rho g}}\left[\frac{4\beta}{4+\lambda} - \frac{\rho R^2}{2+\lambda}\right] \cdot \Omega^2 + \mathrm{O}(\Omega^4) \tag{3}$$

where h_0 is the static climb due to the liquid surface tension γ, ρ is the fluid density, R is the rod radius, $\lambda = R\sqrt{\rho g/\gamma}$ and g is gravitational acceleration. β, named climbing constant, is the linear combination of the first and second normal stress coefficients at zero shear rate (Ψ_{10} and Ψ_{20}).

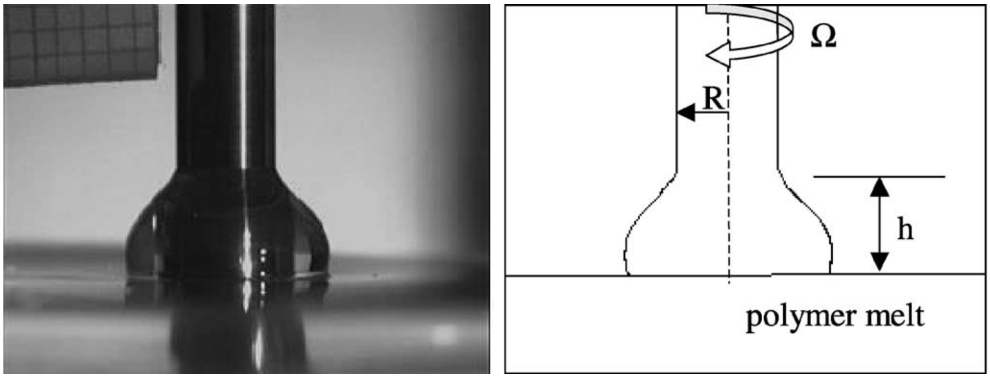

Fig. 1. Representation of the Weissenberg effect: rod-climb image and its digitalization.

$$\beta = \frac{\Psi_{10}}{2} + 2\Psi_{20} \tag{4}$$

Ω is the rod angular velocity in rps; $O(\Omega^4)$ indicates terms of higher order, vanishing in the slow velocity regime.

The intrinsic difficulty in the practical application of this method is related to the accuracy in the measure of the height of climb, as a function of rod rotational speed. As a matter of facts, if only negligible $h - h_0$ values are detected in the slow rotational rate regime, when a quadratic dependence should be observed between h and rotation rate, no reliable measurement can be obtained. When the height of climb value is determined, Eq. (3) can be used to calculate the climbing constant β. Data of the first normal stress coefficient can be independently obtained with the use of conventional shear rheometers. Consequently, in principle, rod-climbing measurements can be used to evaluate, by Eq. (4), the second normal stress coefficient Ψ_{20}. A number of rod-climbing experiments are reported in literature, which were applied to investigate the rheological behavior of polymer melts and solutions [16–18].

2. Experimental

2.1. Materials, PDMS fractions

Linear PDMS with known average molecular parameters were prepared starting from four commercial samples of polydisperse PDMS with viscosities of about 20 000, 30 000, 100 000 and 600 000 cSt. The materials were received from different sources: PDMS 30 and PDMS 100 are chemical grade materials from Aldrich, PDMS 20 and PDMS 600 are industrial products from Polymerland and from Dow Corning respectively; the numbers refer to the material viscosity. Two of the samples, namely PDMS 20 and PDMS 100, were employed in a fractional precipitation, according to a procedure similar to that suggested by Flory [19], to obtain fractions with different molecular weight and reduced polydispersity. The polymer was dissolved in large amount of ethylacetate (EA) solvent and was partially precipitated by adding methanol at 30 °C. In order to reach sufficient amounts of materials to be employed in rheological tests in a reasonable period of time, the initial concentration of EA solutions was set at 7%, a value higher than suggested by the original procedure. The obtained fractions were subsequently refractionated from 2% solutions to obtain materials with different average molecular weights. This allowed to obtain amounts of 18–20 g of polymer fractions with polydispersity narrower than that of the original polymer, although with values which cannot be yet considered as monodisperse. All the obtained materials were characterized by GPC to determine molecular weight and polydispersity index. The analyses were carried out using an apparatus equipped with four 'Ultrastyragel' columns (by Waters) of 10^6, 10^5, 10^4, 500 Å porosity, in toluene at 25 °C. Ten narrow fractions of polystyrene (M_n from 8000 to 174 000, $M_w/M_n < 1.1$) were used as calibration samples, to convert retention volumes (V_r) into molecular weights by applying the universal calibration method. For this purpose the following relations were applied, as referred in literature [20]: $[\eta] = 8.28 \times 10^{-5} M_w^{0.72}$ for polydimethylsiloxane, $[\eta] = 1.29 \times 10^{-4} M_w^{0.71}$ for polystyrene.

Finally, the overall calibration curve had the following form:

$$\mathrm{Log}([\eta]M_w) = 32.3 - 1.99 \cdot V_r + 5.43^{-2} \cdot V_r^2 - 5.97^{-4} \cdot V_r^3$$

Eight fractions of PDMS were selected for further characterization together with the raw polymers. Table 1 reports the measured molecular parameters of these materials. The critical molecular weight M_c of PDMS was estimated in the range of 30 000–38 000 g/mol

Table 1
Measured molecular parameters of PDMS and their fractions

	M_n	M_w	I
PDMS 20	33 100	106 000	3.20
PDMS 30	35 000	117 700	3.36
PDMS 100	44 400	151 700	3.42
PDMS 600	43 000	242 800	5.64
FR1	159 600	230 900	1.45
FR2	128 300	201 200	1.57
FR3	106 200	175 000	1.65
FR4	100 500	156 900	1.56
FR5	85 200	113 900	1.34
FR6	126 400	161 900	1.28
FR7	113 100	143 300	1.27
FR8	89 000	108 900	1.22

M_n and M_w are the number average and the weight average molecular weight respectively; I is the polydispersity index.

[21,22]; all fraction tested had molecular weight values consistently higher than M_c.

2.2. Rheological measurements

Complex shear viscosity and first normal stress coefficient of all materials were determined by oscillatory tests in the low frequency range at 20 and 35 °C by a Rheometrics RDA II and a Rheometrics SR 200 with a 40 mm diameter parallel plate geometry. Tests at 27 °C were also performed with starting materials. In some cases, in order to extend the measurable range to lower frequencies, a concentric cylinders geometry (Couette) was also employed. A 25 mm diameter and 32 mm length bob was used. The obtained curves always resulted to well overlap to those measured in parallel plate geometry tests. A frequency range between 1 and 100 rad/s was investigated. Approaching the lowest test frequencies, all materials showed the presence of a plateau complex viscosity, which, on the basis of the Cox–Merz rule, was assumed as zero shear viscosity. Only in the case of the highest M_w (PDMS 600) a non-negligible variation of viscosity was observed. Fig. 2 shows as example the viscosity curves at 20 °C of the starting materials.

As shown by Coleman and Markovitz [23], Ψ_1 can be estimated in the low shear rate range by dynamic shear tests, being related to G' by the following relationship:

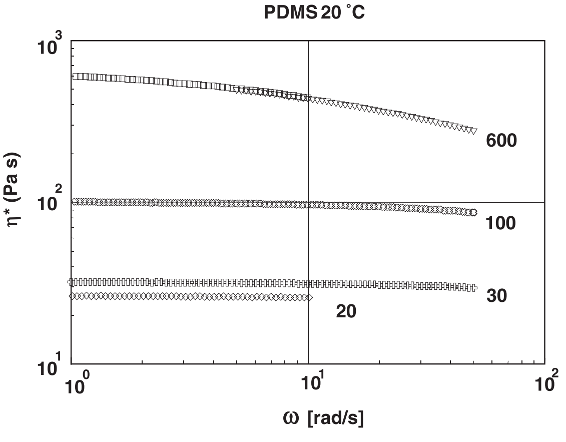

Fig. 2. Complex viscosity curves of unfractionated PDMS.

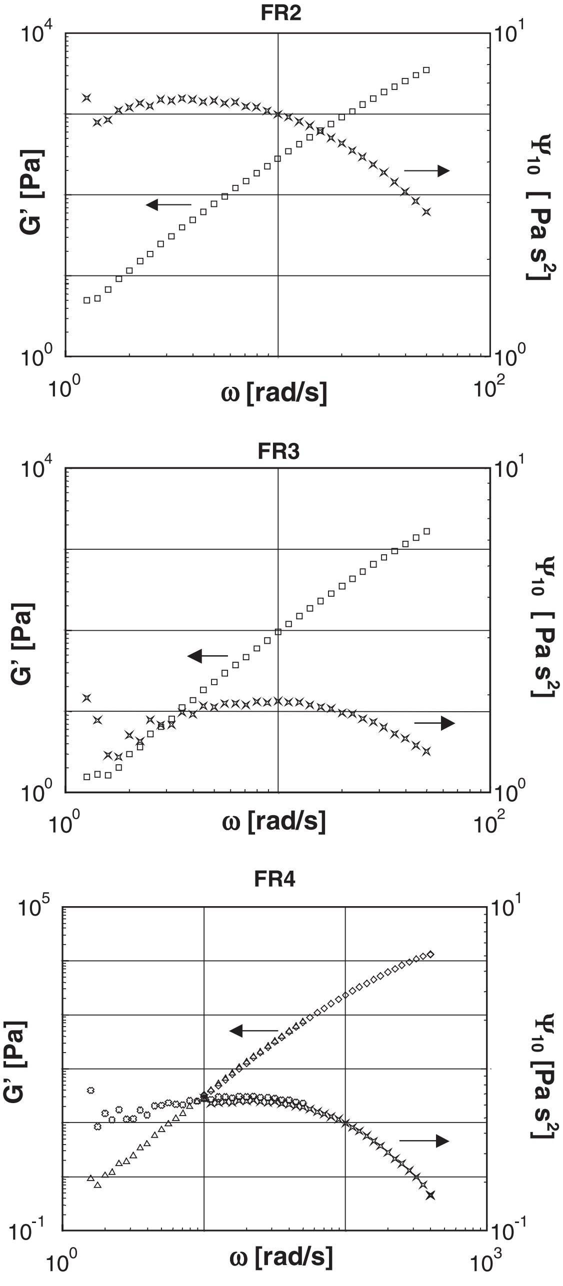

Fig. 3. G', Ψ_1 vs. ω curves of FR2, FR3 and FR4 PDMS fractions.

$$\Psi_1(\dot{\gamma}) = 2G'/\omega^2 \quad \text{with } \dot{\gamma} = \omega \tag{5}$$

Again, all the polymers presented a plateau Ψ_1 region in the low test frequencies, with the exception of PDMS 600, for which a decrease of Ψ_1 with ω even in the lowest test range was observed. In some cases, due to sensor sensitivity limit, the very low frequency data resulted highly dispersed and were therefore discarded. Fig. 3 shows the G', Ψ_1, ω curves of FR2, FR3 and FR4 as examples.

2.3. Weissenberg effect

For the evaluation of the Weissenberg effect and the liquid rise, a rotational rod rheometer with a videocamera for the acquisition of the liquid surface profile was developed. A PC controlled Mavilor brushless motor capable of very low rotation rate with practically no rate oscillations was employed. Rods with 2, 4 and 8 mm diameter and 50 mm length were centered on the motor shaft. The fluid containers consisted of glass cylinders with diameters from 35 to 70 mm. Different diameters were employed to check for possible boundary effects. Such effects are expected to become negligible for container to rod diameter ratio higher than 10 [24]. The fluid surface image was recorded and measured during rod rotation by a COHU videocamera mounted on a low magnification (4–40×) OLYMPUS microscope and connected to an image acquisition system. The images were converted into digital profiles by a Matlab computer code for more accurate measurements (Fig. 1).

The fluid temperature was maintained constant at 20 °C or 35 °C by a thermostatic bath. All materials were degassed under vacuum before tests.

The surface tension of the fluids was measured by the pendant drop method [25]. All the results were within 16 ± 0.5 mJ/m^2. An average value of 16 mJ/m^2 was assumed.

3. Results and discussion

The $\log \eta_0$ results for the starting materials and for the PDMS fractions, which have a relatively narrow molecular weight distribution, were plotted against $\log \overline{M}_w$. As expected the data fit with satisfactory approximation the well-known power function $\eta_0 = k\overline{M}_w^{\alpha}$ with α equal to 3.5 (Fig. 4). In all cases however a very limited, if any, influence of polydispersity over zero shear viscosity was observed. A slightly better fit was observed, for the starting PDMS, when polydispersity index was considered by applying Eq. (1), although with a δ value well below 0.5. For the fractions, which have a polydispersity index in the range 1.22–1.65, the term I^{δ} is practically ineffective for $\delta < 0.5$ and little information can result from experimental data.

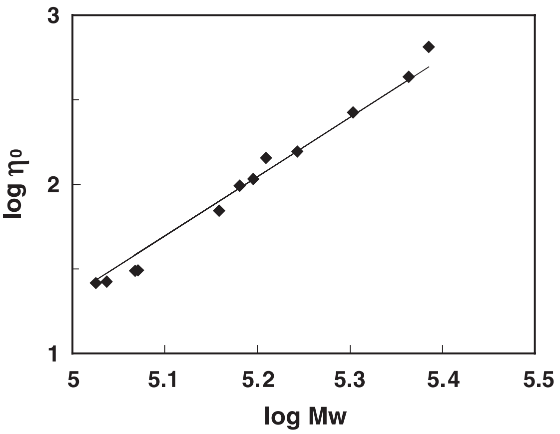

Fig. 4. Zero shear viscosity as function of molecular weight of PDMS at 20 °C (slope 3.5).

On the contrary, as already noted, a marked influence of I over the first normal stress coefficient Ψ_{10} is to be expected if the rheological behavior conforms to the prediction of Eq. (2). This was confirmed by experimental results. However, by applying Eq. (2) to all experimental data at 35 °C, it was observed that an approximate fit could be obtained only if PDMS fractions and starting materials were analyzed separately, therefore assuming for the two sets of data, two different k' values (Fig. 5). On the other hand, k' should be a material constant, independent of I or $\overline{M}_w$. When considering experimental results all together, it was found that the dependence of Ψ_{10} over I seems to be sensibly lower than predicted by Eq. (2); an almost perfect fit was found by applying the following empirical equation (Fig. 6):

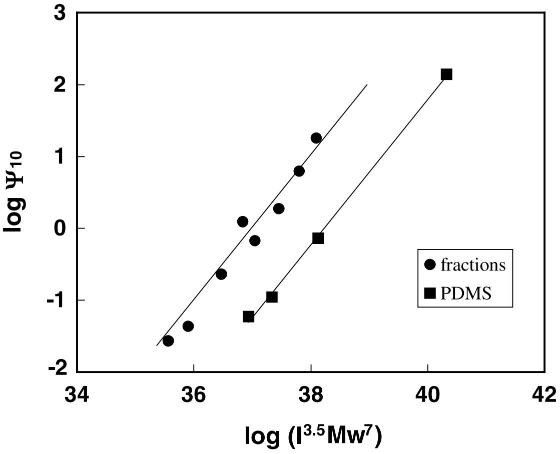

Fig. 5. Ψ_{10} of PDMS and fractions plotted according to Eq. (2).

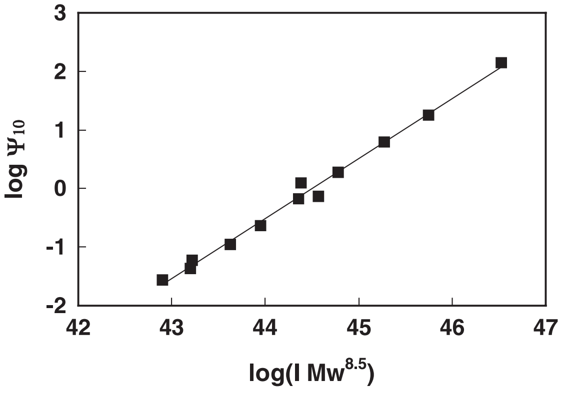

Fig. 6. Ψ_{10} of PDMS and fractions plotted according to Eq. (6).

$$\Psi_{10} = k'\overline{M}_{\mathrm{w}}^{8.5} \cdot I \tag{6}$$

suggesting a linear dependence of Ψ_{10} on polydispersity.

In case of the starting polymers Ψ_{10} was measured at three different temperatures (20, 27, 35 °C). Although the temperature range investigated was quite limited, the results seem in agreement with an Arrhenius type dependence of Ψ_{10} on absolute temperature [26]:

$$\Psi_{10}(T) = B\exp(E_{\mathrm{a}}/RT) \tag{7}$$

Table 2 compares the experimental and the calculated Ψ_{10} values, assuming for the activation energy E_{a} a value of 6500 cal/mol. It can be observed that only in the case of PDMS 600 a certain discrepancy is observed; however, as cited before, in such case the actual Ψ_{10} plateau was not reached, and the experimental data measured are probably an underestimation of actual Ψ_{10} value.

Table 2
Comparison between experimental Ψ_{10} and values calculated according to Eq. (7)

	Temperature (°C)	Experimental Ψ_{10} (Pa s^2)	Calculated Ψ_{10} (Pa s^2)
PDMS 20	20	0.081	0.081
PDMS 20	27	0.065	0.062
PDMS 20	35	0.049	0.047
PDMS 30	20	0.191	0.192
PDMS 30	27	0.149	0.148
PDMS 30	35	0.110	0.111
PDMS 100	20	1.52	1.53
PDMS 100	27	1.16	1.18
PDMS 100	35	0.856	0.887
PDMS 600	20	281	282
PDMS 600	27	180	218
PDMS 600	35	138	164

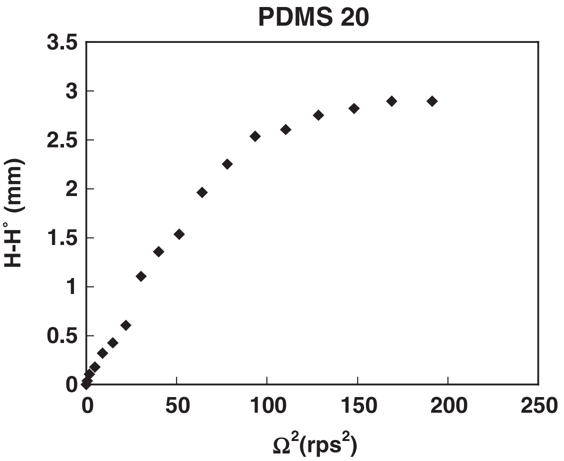

Fig. 7. Height of climb of PDMS 20 at 35 °C as function of rotation rate in a Weissenberg experiment.

The surface profile of all PDMS fluids in rotational rod experiments, were recorded at different rod rotation rates. In case of a isotropic fluid, with "fading memory", which shows a second-order flow regime at low deformation rates, a linear dependence of climb height vs. Ω^2 is expected (Eq. (3)). Deviation from linearity occurs at high Ω values. The limit of such linear behavior cannot be defined "a priori", but should be judged on the basis of experimental observations [18]. The explored rotational rate range was between 0 and 13.8 rps ($\Omega^2 =$ 0–191.4 rps^2). Fig. 7 shows the results for PDMS20 at 35 °C as example. The slope of the linear portion of the curve was determined by a least square interpolation and the climbing constant β of Eq. (3) was calculated. In case of the starting materials, for which larger amounts were available, tests at different temperatures and with different rod/container diameters were carried out (Table 3). As suggested by Eq. (4) no marked effect of rod and/or container diameter over measured β was registered; it should be noted, however, that container to rod diameter ratios higher than 8.75 were always employed i.e. close or higher than the minimum limit (10:1) indicated for reliable measurements [24]. On the other hand a marked influence of molecular weight is evident. The results show that such dependence is due both to variation of Ψ_{10} and Ψ_{20}. Experimental determinations have been reported in literature, indicating that, in polymer melts, Ψ_{20} assumes negative values, and it is an order of magnitude smaller than Ψ_{10} in absolute terms ($-\Psi_{20}/\Psi_{10} = 0$–0.3). Fig. 8 shows the measured $-\Psi_{20}/\Psi_{10}$ ratio as function of $\overline{M}_{\mathrm{w}}$: although dispersed

Table 3
Results of the Weissenberg experiments

	$R_{\text{cont.}}/R_{\text{rod}}$	β (Pa s^2)	Ψ_{10} (Pa s^2)	$-\Psi_{20}$ (Pa s^2)	$-\Psi_{20}/\Psi_{10}$
PDMS 20 (20 °C)	25	0.0236	0.081	0.0083	0.104
PDMS 20 (20 °C)	12.5	0.0236	0.081	0.0083	0.104
PDMS 20 (20 °C)	9.375	0.0245	0.081	0.0079	0.098
PDMS 20 (35 °C)	17.5	0.0172	0.049	0.0035	0.073
PDMS 20 (35 °C)	8.75	0.0189	0.049	0.0027	0.056
PDMS 30 (20 °C)	25	0.0732	0.191	0.0112	0.058
PDMS 30 (20 °C)	12.5	0.0700	0.191	0.0127	0.067
PDMS 100 (20 °C)	25	0.482	1.52	0.139	0.091
PDMS 100 (20 °C)	37.5	0.456	1.52	0.152	0.100
PDMS 100 (20 °C)	18.75	0.559	1.52	0.100	0.066
PDMS 100 (20 °C)	12.5	0.378	1.52	0.191	0.126
PDMS 100 (20 °C)	9.375	0.452	1.52	0.154	0.101
PDMS 100 (35 °C)	17.5	0.335	0.86	0.123	0.143
PDMS 600 (20 °C)	25	61.3	281	39.6	0.141
PDMS 600 (20 °C)	12.5	58.5	281	41.0	0.146
PDMS 600 (20 °C)	9.375	53.8	281	43.4	0.154
PDMS 600 (35 °C)	17.5	16.9	138	26.0	0.189
FR1 (35 °C)	17.5	3.89	17.9	2.52	0.141
FR2 (35 °C)	17.5	2.31	6.19	0.39	0.064
FR3 (35 °C)	17.5	0.495	1.88	0.22	0.118
FR4 (35 °C)	17.5	0.179	0.667	0.078	0.118
FR5 (35 °C)	17.5	0.0135	0.043	0.004	0.093
FR6 (35 °C)	17.5	0.294	1.24	0.16	0.132
FR7 (35 °C)	17.5	0.0821	0.235	0.018	0.075
FR8 (35 °C)	17.5	0.0114	0.027	0.001	0.038

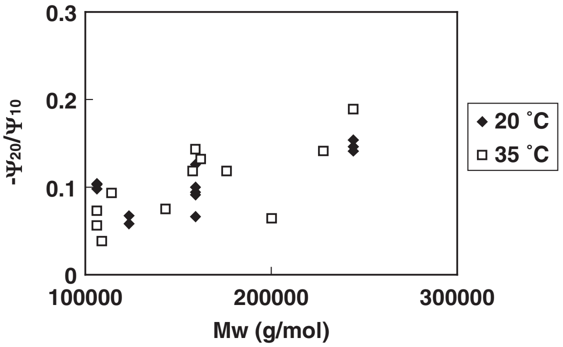

Fig. 8. ($-\Psi_{20}/\Psi_{10}$) ratio as function of M_w of all PDMS (fractions and unfractionated materials).

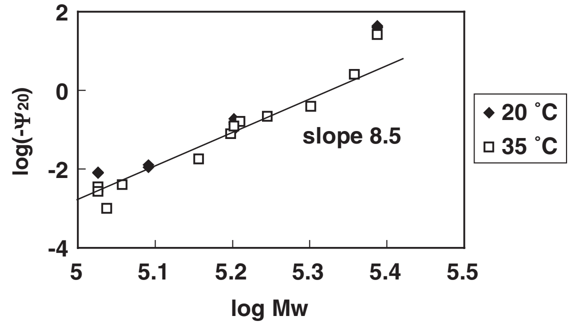

Fig. 9. Ψ_{20} of PDMS and fractions as function of molecular weight.

values are observed, a fairly constant ratio results, with at most, a slightly increasing trend ($a - \Psi_{20}/\Psi_{10}$ vs. $\overline{M}_w$ slope as low as 5×10^{-7} (mol/g) was estimated). This suggests that also for Ψ_{20} a functional dependence on $\overline{M}_w$ similar to that indicated for Ψ_{10} (Eq. (6)) seems adequate; in Fig. 9 the dependence of Ψ_{20} on $\overline{M}_w$ is shown. It should be noted however that, although the polydispersity probably has effect over Ψ_{20} behavior, the uncertainty in the experimental results do not allow to evidence possible influence of I over Ψ_{20}.

4. Conclusions

The rheological functions of a series of linear PDMS polymer with different molecular weight and mol. wt. distribution are measured by means of rotational rheometers. The zero shear viscosity of these materials is well described by a functional dependence on the power 3.5 of molecular weight, while negligible effect of polydispersity was found in these materials. On the contrary, a marked influence of both molecular weight and molecular weight distribution over the first normal stress coefficient is observed. The results appear to deviate from existing empirical equations. A different empirical equation relating Ψ_{10} to molecular weight and polydispersity is therefore proposed.

A rotation rod apparatus is set to measure the second normal stress coefficient based on the Weissenberg effect. Yet considering the experimental uncertainties, the second normal stress coefficient seems to follow a functional dependence on molecular weight similar to that applicable to the first normal stress coefficient Ψ_{10}. This suggests that the second to first normal stress ratio should be fairly independent of molecular weight. Further analysis of results, based on the reptation theory, may give a better insight of the relationship between molecular structure and rheological behavior.

Acknowledgements

The authors gratefully acknowledge the help of Dr. Mendichi, G. Clerici, M.R. Pagano and M. Gullo in the experimental measurements.

References

[1] Bird RB, Armstrong RC, Hassager O. In: Dynamics of polymeric liquids, vol. 1. Wiley; 1977.
[2] Macosko CW. Rheology, principles, measurements and applications. Wiley, VCH; 1994.
[3] Ferry DJ. Viscoelastic properties of polymers. third ed. New York: John Wiley & Sons; 1980.
[4] Graessley WW. Adv Polym Sci 1974;16:1.
[5] Locati G, Gargani L. J Polym Sci, Polym Lett Ed 1973; 11:95.
[6] Friedman EM, Porter RS. Trans Soc Rheol 1975;19:493.
[7] Nichetti D, Manas-Zloczower I. J Rheol 1998;49:951.
[8] Dealy JM, Vu TKP. J Non-Newt Fluid Mech 1977;3:127.
[9] Gao HW, Ramachandran S, Christiansen EB. J Rheol 1981;25:213.
[10] Minoshima W, White JL, Spruiell JE. Polym Eng Sci 1980;20:1166.
[11] Marrucci G, Grizzuti N. J Non-Newt Fluid Mech 1986; 24:127.
[12] Joseph DD, Beavers GS, Fosdick RL. Arch Rat Mech Anal 1973;49:381.
[13] Liao TY, Hu HH, Joseph DD. J Non-Newt Fluid Mech 1994;51:111.
[14] Nunez GA, Ribeiro GS, Arney MS, Feng J, Joseph DD. J Rheol 1994;38:5.
[15] Weissenberg K. Nature 1947;159:310.
[16] Lodge AS, Schieber JD, Bird RB. J Chem Phys 1988; 88:4001.
[17] Hu HH, Riccius O, Chen KP, Arney M, Joseph DD. J Non-Newt Fluid Mech 1990;35:287.
[18] Magda JJ, Lou J, Baek SG. Polymer 1991;32:2000.
[19] Flory PJ. Principles of polymer chemistry. Cornell University Press; 1953.
[20] Haug A, Meyeroff G. Makromol Chem 1962;53:91.
[21] Porter RS, Jonson JF. Chem Rev 1966;66:1.
[22] Mills NJ. Eur Polym J 1969;5:675.
[23] Coleman BD, Markovitz H. J Appl Phys 1966;35:1.
[24] Joseph DD, Beavers GS, Cers A, Dewald C, Hoger A, Than PT. J Rheol 1984;28:325.
[25] Wu S. Polymer interfaces and adhesion. New York: Marcel Dekker; 1982.
[26] Pena JJ, Guzman GM, Santamaria A. Eur Polym J 1981; 18:379.